UNIVERSITÉ DE GENÈVE

Archive ouverte UNIGE
https://archive-ouverte.unige.ch

Article scientifique | Article | 2024

Published version | Open Access

This is the published version of the publication, made available in accordance with the publisher's policy.

St. John's wort extract with a high hyperforin content does not induce P-glycoprotein activity at the human blood-brain barrier

El Biali, Myriam; Wölfl-Duchek, Michael; Jackwerth, Matthias; Mairinger, Severin; Weber, Maria; Bamminger, Karsten; Poschner, Stefan; Rausch, Ivo; Schindler, Natalie; Lozano, Irene Hernández; Jäger, Walter; Nics, Lukas; Tournier, Nicolas; Hacker, Marcus [**and 3 more**]

How to cite

EL BIALI, Myriam et al. St. John's wort extract with a high hyperforin content does not induce P-glycoprotein activity at the human blood-brain barrier. In: Clinical and translational science, 2024, vol. 17, n° 5, p. e13804. doi: 10.1111/cts.13804

This publication URL: https://archive-ouverte.unige.ch/unige:178286

Publication DOI: 10.1111/cts.13804

© The author(s). This work is licensed under a Creative Commons Attribution-NonCommercial (CC BY-NC 4.0) https://creativecommons.org/licenses/by-nc/4.0

Check for updates

Received: 22 February 2024 | Revised: 4 April 2024 | Accepted: 11 April 2024

DOI: 10.1111/cts.13804

ARTICLE

St. John's wort extract with a high hyperforin content does not induce P-glycoprotein activity at the human blood–brain barrier

Myriam El Biali[1,2] | **Michael Wölfl-Duchek**[1,3] | **Matthias Jackwerth**[1] | **Severin Mairinger**[1,3] | **Maria Weber**[1] | **Karsten Bamminger**[3] | **Stefan Poschner**[4] | **Ivo Rausch**[5] | **Natalie Schindler**[3] | **Irene Hernández Lozano**[1] | **Walter Jäger**[4] | **Lukas Nics**[3] | **Nicolas Tournier**[6] | **Marcus Hacker**[3] | **Markus Zeitlinger**[1] | **Martin Bauer**[1] | **Oliver Langer**[1,3]

[1]Department of Clinical Pharmacology, Medical University of Vienna, Vienna, Austria

[2]Division of Clinical Pharmacology and Toxicology, Geneva University Hospitals, Geneva, Switzerland

[3]Department of Biomedical Imaging und Image-guided Therapy, Division of Nuclear Medicine, Medical University of Vienna, Vienna, Austria

[4]Department of Pharmaceutical Sciences, University of Vienna, Vienna, Austria

[5]QIMP Team, Center for Medical Physics and Biomedical Engineering, Medical University of Vienna, Vienna, Austria

[6]Laboratoire d'Imagerie Biomédicale Multimodale (BIOMAPS), Université Paris-Saclay, CEA, CNRS, Inserm, Service Hospitalier Frédéric Joliot, Orsay, France

Correspondence
Oliver Langer, Department of Clinical Pharmacology, Division of Clinical Pharmacokinetics and Imaging, Medical University of Vienna, Währinger-Gürtel 18-20, 1090 Vienna, Austria.
Email: oliver.langer@meduniwien.ac.at

Abstract

St. John's wort (SJW) extract, a herbal medicine with antidepressant effects, is a potent inducer of intestinal and/or hepatic cytochrome P450 (CYP) enzymes and P-glycoprotein (P-gp), which can cause clinically relevant drug interactions. It is currently not known whether SJW can also induce P-gp activity at the human blood–brain barrier (BBB), which may potentially lead to decreased brain exposure and efficacy of certain central nervous system (CNS)-targeted P-gp substrate drugs. In this study, we used a combination of positron emission tomography (PET) imaging and cocktail phenotyping to gain a comprehensive picture on the effect of SJW on central and peripheral P-gp and CYP activities. Before and after treatment of healthy volunteers ($n = 10$) with SJW extract with a high hyperforin content (3–6%) for 12–19 days (1800 mg/day), the activity of P-gp at the BBB was assessed by means of PET imaging with the P-gp substrate [^{11}C]metoclopramide and the activity of peripheral P-gp and CYPs was assessed by administering a low-dose phenotyping cocktail (caffeine, omeprazole, dextromethorphan, and midazolam or fexofenadine). SJW significantly increased peripheral P-gp, CYP3A, and CYP2C19 activity. Conversely, no significant changes in the peripheral metabolism, brain distribution, and P-gp-mediated efflux of [^{11}C]metoclopramide across the BBB were observed following the treatment with SJW extract. Our data suggest that SJW does not lead to significant P-gp induction at the human BBB despite its ability to induce peripheral P-gp and CYPs. Simultaneous intake of SJW with CNS-targeted P-gp substrate drugs is not expected to lead to P-gp-mediated drug interactions at the BBB.

Myriam El Biali, Michael Wölfl-Duchek and Matthias Jackwerth contributed equally to this study (shared first authors).

This is an open access article under the terms of the Creative Commons Attribution-NonCommercial License, which permits use, distribution and reproduction in any medium, provided the original work is properly cited and is not used for commercial purposes.
© 2024 The Authors. *Clinical and Translational Science* published by Wiley Periodicals LLC on behalf of American Society for Clinical Pharmacology and Therapeutics.

Study Highlights

WHAT IS THE CURRENT KNOWLEDGE ON THE TOPIC?

St. John's wort (SJW) can lead to clinically relevant drug interactions due to induction of intestinal/hepatic P-glycoprotein (P-gp) and CYP enzymes. It is not known whether SJW can also induce P-gp activity at the human blood–brain barrier (BBB), which may lead to decreased brain exposure and efficacy of CNS-targeted P-gp substrate drugs.

WHAT QUESTION DID THIS STUDY ADDRESS?

We used a combination of PET imaging with the P-gp substrate [^{11}C]metoclopramide and cocktail phenotyping to assess the effect of treatment with SJW extract on central and peripheral P-gp and CYP activities in healthy volunteers.

WHAT THIS STUDY ADDS TO OUR KNOWLEDGE?

Despite induction of peripheral P-gp, CYP3A and CYP2C19, no significant changes in the peripheral metabolism, brain distribution and efflux of [^{11}C]metoclopramide across the BBB were observed.

HOW THIS MIGHT CHANGE CLINICAL PHARMACOLOGY OR TRANSLATIONAL SCIENCE?

Our data suggest that SJW does not lead to P-gp induction at the human BBB, despite its ability to induce peripheral P-gp and CYPs. Simultaneous intake of SJW with CNS-targeted P-gp substrate drugs is not expected to lead to P-gp-mediated drug interactions at the BBB.

INTRODUCTION

Herbal medicines containing extracts from the plant St. John's wort (SJW; *Hypericum perforatum* L.) such as WS® 5570 are widely used to treat mild-to-moderate depression.[1] SJW products are broadly available over the counter and are often used as co-medication with prescription drugs. SJW extracts contain numerous components belonging to different chemical classes, with hypericin, hyperforin, and quercetin as the main components.[2] It was initially suggested that hyperforin was the major active principle of SJW leading to antidepressant effects, but clinical efficacy has also been demonstrated with SJW extracts with a low hyperforin content.[2]

Hyperforin is a powerful activator of the human pregnane X receptor (PXR),[3] a ligand-activated nuclear receptor, which transcriptionally regulates the expression of cytochrome P 450 (CYP) enzymes (e.g., CYP3A4, CYP2B6, CYP2C9, and CYP2C19) as well as the efflux transporter P-glycoprotein (P-gp, encoded in humans by the *ABCB1* gene and in rodents by the *Abcb1a/b* genes). Intake of SJW can cause clinically relevant interactions with drugs that are metabolized by CYP enzymes and/or those that are substrates of P-gp. Clinical studies showed that hyperforin-containing SJW preparations can induce P-gp and CYP3A activity at the level of the intestinal epithelium, leading to decreased systemic absorption of substrate drugs such as digoxin, fexofenadine, and cyclosporin A.[4–8] Similarly, induction of hepatic CYP activity can lead to increased metabolic clearance and decreased plasma exposure of substrate drugs.

Besides the intestinal epithelium, P-gp is abundantly expressed at the blood–brain barrier (BBB), where it can limit the brain penetration of substrate drugs. Preclinical studies showed that the brain distribution of several central nervous system (CNS)-targeted drugs, such as antidepressants (e.g., citalopram, fluoxetine, fluvoxamine, nortriptyline, paroxetine, and venlafaxine), antipsychotics (e.g., chlorpromazine, clozapine, haloperidol, risperidone, and sulpiride), antiepileptic drugs (phenytoin), and opioids (morphine, hydrocodone), is enhanced in *Abcb1a/b*$^{(-/-)}$ mice relative to wild-type mice, suggesting P-gp-mediated efflux transport at the BBB.[9] Numerous studies demonstrated that PXR activation can induce P-gp activity at the rodent or porcine BBB.[10–13] However, considerable species differences exist in the pharmacological activation profile of PXR[14] and it is incompletely understood whether P-gp activity can be induced at the human BBB in vivo. P-gp induction at the human BBB may increase P-gp-mediated efflux transport of CNS-targeted P-gp substrate drugs. This may lead to decreased CNS exposure, despite plasma concentrations in the therapeutic range, and potentially lower therapeutic efficacy. On the other hand, P-gp induction may also be therapeutically exploited in order to enhance the brain clearance of endogenous neurotoxic compounds, such as beta-amyloid (Aβ) peptides.[11]

17520062, 2024, 5, Downloaded from https://ascpt.onlinelibrary.wiley.com/doi/10.1111/cts.13804 by Bibliotheque de l'Universite de Geneve, Division de l'Information, Wiley Online Library on [26/06/2024]. See the Terms and Conditions (https://onlinelibrary.wiley.com/terms-and-conditions) on Wiley Online Library for rules of use; OA articles are governed by the applicable Creative Commons License

While intestinal P-gp-mediated drug interactions can be straightforwardly assessed by analyzing the plasma pharmacokinetics of victim drugs,[15] P-gp-mediated drug interactions at the BBB do not manifest themselves in changes in plasma pharmacokinetics and require the measurement of intracerebral pharmacokinetics. The minimally invasive imaging technique positron emission tomography (PET) can be used to assess P-gp-mediated drug interactions at the human BBB by measuring the brain concentrations of radiolabeled P-gp substrates.[16]

In this study, we used PET imaging with the P-gp substrate [^{11}C]metoclopramide[17] to assess the effect of treatment with SJW extract with a high hyperforin content (3–6%) on P-gp activity at the BBB of healthy volunteers. Furthermore, peripheral P-gp and CYP activities were measured by administering a phenotyping cocktail containing low doses of P-gp and CYP substrate drugs.

METHODS

This study was conducted in accordance with the ICH-GCP guidelines and the Declaration of Helsinki. The trial was registered in the EudraCT database as a phase I study (EudraCT number 2017-000989-30) and was approved by the Ethics Committee of the Medical University of Vienna and the Austrian Agency for Health and Food Safety. All subjects gave oral and written informed consent before enrollment in the study. Ten subjects (2 women, mean age: 32 ± 13 years, mean weight: 80 ± 9 kg) were included into the study. Subjects were required to be >18 years old and non-smokers. Subjects receiving SJW or rifampicin during 2 weeks before the start of the study or having a previous history of drug or alcohol abuse were excluded from the study. Food or beverages that contain methylxanthines were not permitted 12 h before the PET study days and 24 h before phenotyping. The consumption of any food or drinks containing grapefruit was not permitted throughout the study. Female participants taking hormonal contraceptives were informed about the potential for decreased effectiveness with SJW. Subjects were judged as healthy based on clinical examination and routine blood and urine laboratory assessments.

Study drugs

Neuroplant® 600 mg film-coated tablets were obtained from Dr. Willmar Schwabe GmbH & Co. KG (Karlsruhe, Germany). One film-coated tablet contained 570–630 mg of WS® 5570, a dry extract from SJW (3–7:1) (extraction solvent: 80% (*v*/*v*) methanol), with defined contents of 3–6% hyperforin, 0.1–0.3% hypericin, not less than 6% flavonoids and not less than 1.5% rutin. Two batches were used in this study. The first batch (expiry date 10/2022, #4190620) contained 595 mg Hypericum extract including 29.3 mg hyperforin per tablet (used for subjects 1–6) and the second batch (expiry date 12/2024, #4260822) contained 588 mg hypericum extract including 27.8 mg hyperforin per tablet (used for subjects 7–10). For the phenotyping cocktail, caffeine (Coffekapton® 100-mg tablets, Strallhofer Pharma GmbH, Austria), omeprazole (Omec Hexal® 10-mg capsules; Hexal Pharma GmbH, Austria), dextromethorphan (Wick Formel 44® Hustenstiller-Sirup 20 mg/15 mL; WICK Pharma Zweigniederlassung der Procter & Gamble GmbH, Germany), midazolam (OZASED® 2 mg/mL solution; Primex Pharmaceuticals Oy, Finland), and fexofenadine hydrochloride (Telfast® 30 mg film-coated tablets; Sanofi-Aventis Deutschland GmbH, Germany) were administered. Due to the short radioactive half-life of carbon-11 (20.4 min), [^{11}C]metoclopramide was extemporaneously prepared on each study day and formulated in sterile phosphate-buffered saline solution containing 8.6% (*v*/*v*) ethanol as described before.[18]

Study design

The study was carried out as an explorative pharmacokinetic PET study (phase I study) at the Medical University of Vienna. Study participants underwent two 60-min brain PET scans after intravenous (i.v.) injection of [^{11}C]metoclopramide. Between the first and the second PET scan subjects were treated with SJW tablets (Neuroplant®) at a dose of 1800 mg per day for 12–19 days (median: 15 days). The second PET scan was performed 46 ± 8 h (range: 38–69 h) after intake of the last SJW dose in order to allow for washout of hyperforin and avoid a possible P-gp inhibitory effect.[19] The first two subjects took three 600-mg tablets once daily (in the evening). Due to gastrointestinal side effects (diarrhea and stomach pain), the dosing schedule was adjusted to three administrations per day in the remaining eight subjects. Blood samples (4 mL) for determination of hyperforin plasma concentrations were collected on day 7–8 after start of treatment with SJW extract, at the end of treatment (median: 14 days, range: 12–17 days) and 2 days after end of treatment with SJW extract (i.e., on the day of the second PET scan). Blood was centrifuged to obtain plasma, which was stored at −80°C and protected from light for analysis of hyperforin concentrations as described in the Methods S1.

Eight out of 10 subjects received a previously described phenotyping cocktail[20] orally together with a glass of water (at least 2 h after the last meal) once before, once during (at day 7–8) and once after the end of

17528062, 2024, 5, Downloaded from https://ascpt.onlinelibrary.wiley.com/doi/10.1111/cts.13804 by Bibliotheque de l'Universite de Geneve, Division de l'Information, Wiley Online Library on [26/06/2024]. See the Terms and Conditions (https://onlinelibrary.wiley.com/terms-and-conditions) on Wiley Online Library for rules of use; OA articles are governed by the applicable Creative Commons License

SJW treatment (in the morning of the second PET study day) for assessment of peripheral P-gp and CYP activities. The time difference between cocktail administration and i.v. injection of [^{11}C]metoclopramide was 5.8 ± 2.3 h (range: 1.9–8.1 h). The phenotyping cocktail comprised low doses of caffeine (50 mg), omeprazole (10 mg), dextromethorphan (10 mg), midazolam (1 mg), and fexofenadine hydrochloride (30 mg). Since fexofenadine and midazolam were not deliverable throughout the entire study period, three subjects received caffeine, omeprazole, dextromethorphan, and midazolam, and five subjects received caffeine, omeprazole, dextromethorphan, and fexofenadine. Four capillary whole blood drops were successively collected from single finger pricks at 2, 3, and 6 h (the 3- and 6-h samples were only collected from subjects receiving fexofenadine) after phenotyping cocktail administration using a HemaXis™ DB 10 whole blood collection device (DBS System SA, Switzerland). The blood collection devices were allowed to dry for 30 min and then stored at −20°C until analysis of the phenotyping drugs and their metabolites (Methods S1).

PET/MR imaging and blood sampling

Subjects underwent two PET/magnetic resonance imaging (MRI) brain examinations on a fully-integrated PET/MRI system (Siemens Biograph mMR, Erlangen, Germany). A head and neck coil was used in order to ensure a high signal-to-noise ratio for the MR imaging. Foam cushions were placed inside the MR head coil to minimize involuntary head movement. The integrated PET/MR imaging protocol included a structural T1-weighted image acquired with a magnetization prepared rapid gradient echo (MPRAGE) sequence (echo time/repetition time = 3.75/1.67 ms, inversion time = 950 ms, flip angle = 8°, 192 sagittal slices, voxel size = 1 × 1 × 1 mm) for spatial normalization. Subjects were i.v. injected with a microdose of [^{11}C]metoclopramide (334 ± 41 MBq, containing <20 μg of unlabeled metoclopramide, diluted to a final volume of 10 mL with physiological saline solution) as a slow bolus over 20 s. At the start of the injection, a 60-min list mode PET data acquisition was initiated and arterial blood samples (3 mL) were manually collected approximately every 10 s for the first 2.5 min followed by 9-mL samples at 5, 10, 20, 30, 40, and 60 min after radiotracer injection. Aliquots of blood and plasma were measured for radioactivity in a gamma counter (Packard Cobra II auto-gamma counter; Packard Instrument Company, Meriden, Connecticut, USA), which was cross-calibrated with the PET camera. The plasma samples collected at 10, 20, 30, and 40 min after radiotracer injection were analyzed for radiolabeled metabolites of [^{11}C]metoclopramide with radio-high-performance liquid chromatography (radio-HPLC) as described in detail elsewhere.[17] A mono-exponential decay function was fitted to the percentage of unchanged [^{11}C]metoclopramide in plasma versus time and then applied to the corresponding decay-corrected total radioactivity counts in plasma to derive a metabolite-corrected arterial plasma input function. After the imaging session, subjects were asked to empty their urinary bladder and aliquots of urine were measured for radioactivity in the gamma counter. Decay-corrected urinary radioactivity concentrations were multiplied by the collected urine volume to obtain the percentage of the injected dose (%ID) excreted into urine. Following the PET/MRI examination, the subjects were moved to a PET/CT system (Biograph Vision 600, Siemens Healthineers, Germany), where a low-dose computed tomography (CT) scan (120 kVp, 50 mAs) of the brain was acquired for the purpose of attenuation correction.

Imaging data analysis

The PET list mode data were re-binned into 1 × 15 s, 3 × 5 s, 3 × 10 s, 2 × 30 s, 3 × 60 s, 2 × 150 s, 2 × 300 s and 4 × 600 s frames and each PET frame was reconstructed into a 256 × 256 × 127 matrix (voxel size 1.4 × 1.4 × 2.0 mm^3) with an ordinary Poisson ordered subset expectation maximization algorithm (OP-OSEM, 4 iterations, 21 subsets). A 3 mm FWHM Gaussian post-reconstruction filter was applied to all images. Scatter correction along with a CT-attenuation correction was applied to all PET data. To perform the CT-attenuation correction, the low-dose CT scan was co-registered to the T1-MPRAGE sequence (RS-1) and a bilinear scaling was applied to convert the CT image to a CT-attenuation correction map. The brain kinetics of [^{11}C]metoclopramide were analyzed using a brain region atlas (N30R83) implemented in the PNEURO tool in PMOD (version 4.403; PMOD Technologies Ltd., Zurich, Switzerland). The anatomical MRI was segmented and matched to a template before transferring the atlas regions to the PET data. Regional concentration-time curves were extracted for whole brain gray matter (WBGM), cerebellum, middle frontal gyrus and basal ganglia (comprising left and right caudate nucleus, nucleus accumbens, putamen, thalamus, and pallidum). The kinetic modeling tool PKIN implemented in PMOD was used to analyze the PET and metabolite-corrected plasma data employing a reversible 1-tissue-2-rate constant (1T2K) compartmental model to estimate the rate constants for radioactivity transfer from plasma into brain (K_1, mL/(cm^3 × min)) and from brain into plasma (k_2, 1/min) and the total volume of distribution ($V_T = K_1/k_2$, mL/cm^3).[17] V_T equals the brain-to-plasma concentration ratio of [^{11}C]metoclopramide at

17528062, 2024, 5, Downloaded from https://ascpt.onlinelibrary.wiley.com/doi/10.1111/cts.13804 by Bibliotheque de l'Universite de Geneve, Division de l'Information, Wiley Online Library on [26/06/2024]. See the Terms and Conditions (https://onlinelibrary.wiley.com/terms-and-conditions) on Wiley Online Library for rules of use; OA articles are governed by the applicable Creative Commons License

steady state. The fractional arterial blood volume in the brain (V_b) was included as a fitting parameter.

For display purposes, the brain and metabolite-corrected plasma concentration–time curves were expressed in units of percentage of the injected dose per cm^3 or mL (%ID/cm^3 or %ID/mL). The area under the concentration–time curves (AUC, %ID/cm^3 × min or %ID/mL × min) was calculated using Prism (version 10.1.0; GraphPad Software, La Jolla, CA, USA).

Sample size considerations and statistical analysis

A power analysis was conducted to determine the study sample size using data from our previous study, in which the effect of cyclosporin A was assessed on the brain distribution of [^{11}C]metoclopramide in healthy volunteers.[17] In this study, the coefficient of variation of [^{11}C]metoclopramide V_T in WBGM in presence and absence of cyclosporin A was 15%.[17] Since a difference in [^{11}C]metoclopramide brain distribution of <20% after P-gp induction is unlikely to be clinically significant, we used this as a cutoff for a significant P-gp induction at the human BBB. Under these assumptions, our power analysis indicated that 10 subjects were sufficient to provide 80% power with $\alpha = 0.05$ to detect at least a 20% change in brain distribution of [^{11}C]metoclopramide. Statistical analysis was performed using Prism. After confirmation of the normal distribution of the data using the Shapiro–Wilk normality test, outcome parameters were compared between two conditions using a two-sided, paired or unpaired t-test and between multiple conditions using one-way ANOVA followed by a Dunnett's multiple comparison test. The Pearson's correlation coefficient (r) was calculated to assess correlations. The level of statistical significance was set to a p value of <0.05. All values are given as mean ± standard deviation (SD).

RESULTS

We included 10 subjects into our study. Each subject underwent two brain PET scans after i.v. injection of [^{11}C]metoclopramide: a first baseline scan and a second scan after treatment with SJW extract at a daily dose of 1800 mg for 12–19 days. Adverse events occurring during the study are listed in Table S1. SJW was generally well-tolerated and all recorded adverse events were mild. All subjects underwent arterial blood sampling in parallel to PET imaging to generate metabolite-corrected arterial plasma input functions for kinetic modeling analysis. For one subject (#4), arterial blood sampling was not successful for the second PET scan and the data of this subject were excluded from kinetic modeling analysis.

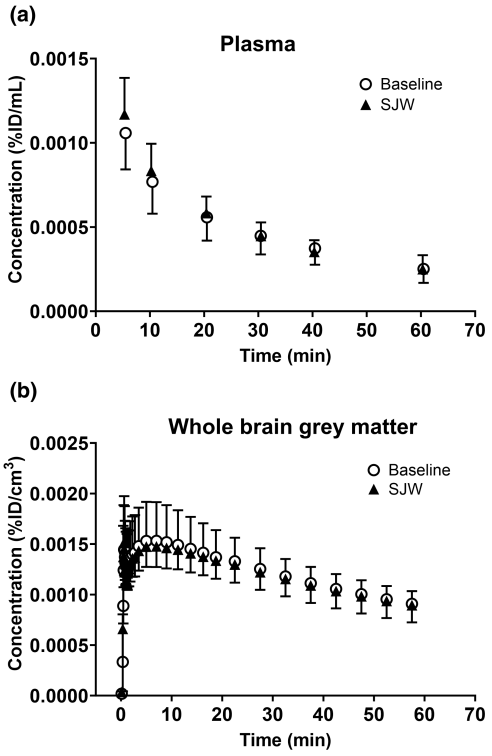

FIGURE 1 Concentration–time curves (mean ± SD) of [^{11}C]metoclopramide in arterial plasma (corrected for metabolites) (a) and whole brain gray matter (b) at baseline ($n = 10$) and after treatment with St. John's wort extract for 12–19 days ($n = 10$).

The arterial plasma concentration-time curves of unchanged [^{11}C]metoclopramide were comparable between the baseline scan and the scan after treatment with SJW extract (Figure 1a). AUC of unchanged [^{11}C]metoclopramide in plasma calculated from 5 to 60 min after radiotracer injection was not significantly different between the two scans (scan 1: 0.026 ± 0.005 %ID/mL × min; scan 2: 0.026 ± 0.004 %ID/mL × min). The percentage of unchanged [^{11}C]metoclopramide in plasma at 40 min after radiotracer injection was not significantly different between the two scans (scan 1: 52 ± 13%; scan 2: 46 ± 18%). The percentage of the administered radioactivity excreted into urine at the end of the scan did not significantly differ between the baseline scan and the scan after SJW treatment (scan 1: 13.1 ± 4.9 %ID; scan 2: 13.6 ± 4.6 %ID).

For the brain, WBGM, cerebellum, middle frontal gyrus, and basal ganglia were analyzed as representative gray matter regions of interest. In Figure 1b, concentration–time curves of [^{11}C]metoclopramide in WBGM are shown at baseline and after treatment with SJW extract and in Figure 2 representative PET average images. Exposure (AUC) to [^{11}C]metoclopramide in WBGM was comparable at baseline and after treatment with SJW extract (scan 1:

17528062, 2024, 5, Downloaded from https://ascpt.onlinelibrary.wiley.com/doi/10.1111/cts.13804 by Bibliotheque de l'Universite de Geneve, Division de l'Information, Wiley Online Library on [26/06/2024]. See the Terms and Conditions (https://onlinelibrary.wiley.com/terms-and-conditions) on Wiley Online Library for rules of use; OA articles are governed by the applicable Creative Commons License

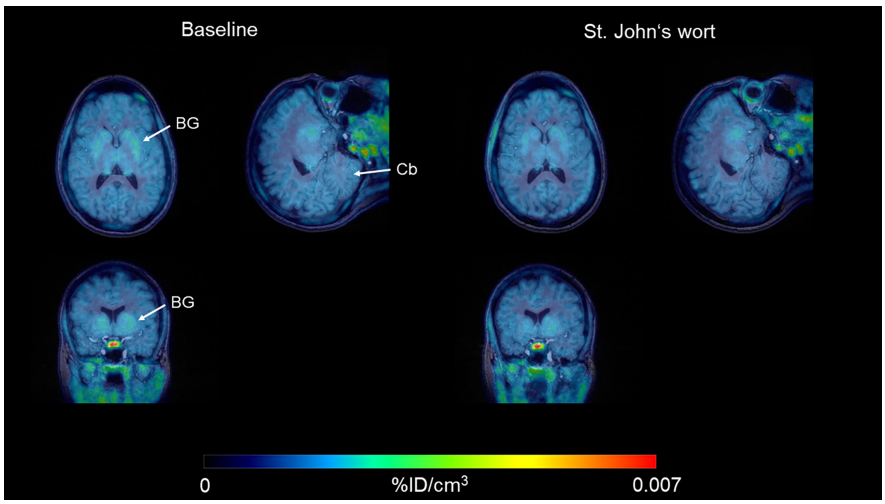

FIGURE 2 Representative MR-co-registered PET average images (4–60 min) for one female subject (#10) at baseline and after treatment with St. John's wort extract for 12 days. Radioactivity concentration is expressed as percentage of the injected dose per cm^3 (%ID/cm^3). The basal ganglia (BG) and cerebellum (Cb) are labeled with arrows.

0.070 ± 0.012 %ID/cm^3 × min; scan 2: 0.069 ± 0.010 %ID/cm^3 × min).

The outcome parameters from kinetic modeling K_1, k_2 and V_T in WBGM are shown in Figure 3 for individual subjects. Mean values of outcome parameters for all examined brain regions are given in Table 1. In none of the brain regions, any significant differences in K_1, k_2, and V_T values could be detected between the two scans. Plasma concentrations of hyperforin were determined at half time and at the end of SJW treatment and at the time of the second PET scan (Table 2). Hyperforin plasma concentrations at the end of SJW treatment ranged from 111 to 362 ng/mL in individual subjects. At the time of the PET scan (i.e., at 2 days after end of SJW treatment), hyperforin plasma concentrations had declined by a factor of 4–20 as compared to respective values at the end of SJW treatment (Table 2). There was no significant correlation between the percentage changes in K_1 ($r = 0.5064$, $p = 0.2004$), k_2 ($r = 0.4388$, $p = 0.2768$) or V_T ($r = -0.09692$, $p = 0.8194$) in scan 2 relative to scan 1 and hyperforin plasma concentrations at the end of SJW treatment (data not shown).

Study participants received a phenotyping cocktail containing low doses of probe substrates for P-gp (fexofenadine) and CYP enzymes before, at day 7–8 and after the end of SJW treatment. Fexofenadine blood concentration–time curves on the three occasions are shown in Figure 4a and the corresponding AUC values in Figure 4b. Fexofenadine blood AUC was significantly lower (−45%) after the end of SJW treatment as compared to baseline. The concentration ratios of metabolite/CYP probe (metabolic ratios) at the 2-h sampling timepoint before, at day 7–8 and after the end of SJW treatment are shown in Figure S1. 5-Hydroxyomeprazole/omeprazole metabolic ratios (CYP2C19) at day 7–8 and after the end of treatment and 1-hydroxymidazolam/midazolam metabolic ratios (CYP3A) at day 7–8 were significantly increased as compared to baseline.

DISCUSSION

In this study, we used a combination of PET imaging with [^{11}C]metoclopramide and cocktail phenotyping to assess the effect of treatment with SJW extract with a high hyperforin content on central and peripheral P-gp activity and peripheral CYP activities in healthy volunteers. Despite induction of peripheral P-gp, no changes in the brain distribution and efflux of [^{11}C]metoclopramide were observed, indicating absence of P-gp induction at the BBB.

Several different radiolabeled P-gp substrates have been described for assessing P-gp activity at the human BBB. These include [^{11}C]*N*-desmethyl-loperamide, racemic or (*R*)-[^{11}C]verapamil, [^{18}F]MC225 and [^{11}C]metoclopramide.[17,21–24] [^{11}C]*N*-desmethyl-loperamide and (*R*)-[^{11}C]verapamil are very efficiently transported by P-gp at the BBB, resulting in very low brain uptake when P-gp is fully functional, and are therefore not ideal probe substrates to detect a P-gp induction at the BBB with PET. Moreover, (*R*)-[^{11}C]verapamil is extensively metabolized by CYP3A enzymes, which are inducible by PXR activation, and forms brain-penetrant radiolabeled metabolites.[25] This further limits the utility of (*R*)-[^{11}C]verapamil to assess the effect of PXR activation on P-gp activity. In contrast, the present study showed that CYP3A induction by SJW did not impact the plasma pharmacokinetics (Figure 1a) and metabolism of [^{11}C]metoclopramide. This is because [^{11}C]metoclopramide is primarily metabolized by CYP2D6,[26] which is not inducible via PXR.[27] This is consistent with preclinical data showing that the potent CYP inducer carbamazepine had no effect on the plasma pharmacokinetics and metabolism of [^{11}C]metoclopramide in rats.[28] Moreover, [^{11}C]metoclopramide lacks brain-penetrant radiolabeled metabolites[29] and shows good passive permeability at the BBB resulting in appreciable brain distribution even when P-gp is fully functional. [^{11}C]Metoclopramide can be considered as a "weak" P-gp substrate,[16] which

17528062, 2024, 5, Downloaded from https://ascpt.onlinelibrary.wiley.com/doi/10.1111/cts.13804 by Bibliotheque de l'Universite de Geneve, Division de l'Information, Wiley Online Library on [26/06/2024]. See the Terms and Conditions (https://onlinelibrary.wiley.com/terms-and-conditions) on Wiley Online Library for rules of use; OA articles are governed by the applicable Creative Commons License

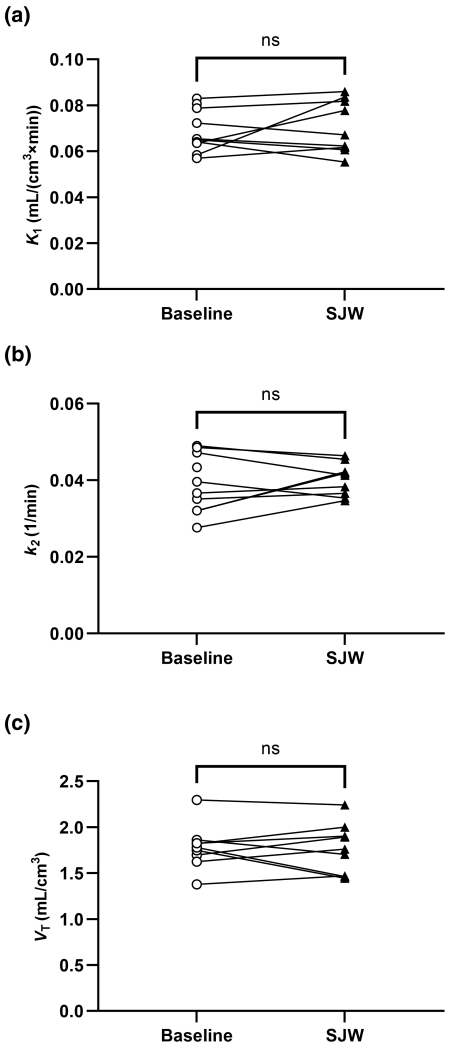

FIGURE 3 Outcome parameters from kinetic modeling (K_1, a; k_2, b; V_T, c) for whole brain gray matter in individual subjects for baseline scans ($n = 10$) and scans after treatment with St. John's wort extract for 12–19 days ($n = 9$). For one subject, arterial blood sampling was not successful for the scan after treatment with St. John's wort extract, so that kinetic modeling analysis was not feasible. ns, not significant; two-sided, paired t-test.

resembles several CNS-targeted drugs with respect to its relatively good brain penetration despite P-gp efflux transport.[9,30] We have previously shown that [^{11}C]metoclopramide is a sensitive radiotracer to measure pharmacological P-gp induction at the mouse BBB after treatment with the rodent PXR ligand 5-pregnen-3β-ol-20-one-16α-carbonitrile.[31]

Numerous commercially available SJW preparations exhibit substantial variability in hyperforin content, influenced by the extraction method.[2] We used in our study SJW tablets containing WS® 5570, a dry extract from SJW (extraction solvent: 80% methanol) with a defined content of 3–6% hyperforin. The recommended daily dose is 600 mg for treatment of mild to moderate depression. We chose a high daily dose of 1800 mg based on results from a phase III study, in which this dose was well-tolerated during a treatment period of 16 weeks in 38 patients suffering from moderate or severe depression.[32] The treatment duration in our study (median: 15 days) was adopted from previous studies.[4–7] At the end of treatment with SJW extract, mean hyperforin plasma concentration was 199 ± 93 ng/mL (371 ± 173 nmol/L) (Table 2). This was approximately two times higher than the average hyperforin plasma concentration (97.3 ± 12.6 ng/mL) reported in healthy volunteers after 8 days of treatment with the same SJW extract at a dose of 900 mg/day[33] and several times above the in vitro half-maximum effect concentration (EC_{50}) of hyperforin for activation of human PXR (23 nmol/L).[3] However, when considering the in silico predicted unbound fraction of hyperforin in plasma published by Adiwidjaja et al. of 0.0005,[34] the unbound hyperforin concentration in plasma (0.19 nmol/L) would be too low to achieve P-gp induction at the human BBB. This is in fact similar to previous investigations showing that the unbound plasma concentrations of clinically used P-gp inhibitors are too low to achieve a great degree of P-gp inhibition at the human BBB.[35]

Since SJW extract and hyperforin inhibit P-gp activity in vitro and in vivo,[6,19] we performed the second PET scan 46 ± 8 h after administration of the last SJW dose, which corresponds to approximately four terminal elimination half-lives of hyperforin (11.2 h).[33] We confirmed that hyperforin plasma concentrations were very low at the time of the PET scan (Table 2), making a P-gp inhibitory effect unlikely.

Concomitant with PET imaging, we used a low-dose phenotyping cocktail containing one P-gp substrate (fexofenadine) and different CYP substrates to simultaneously assess peripheral P-gp and CYP activities. The phenotyping cocktail was a reduced form (containing less probes) of a previously described phenotyping cocktail, which has been validated for detecting P-gp, CYP3A and CYP2C19 induction after treatment of healthy volunteers with the human PXR activator rifampicin.[20] In contrast to the previous study,[20] our subjects were not genotyped for *CYP* and *ABCB1* polymorphisms, which may have added some variability to our phenotyping data. We observed a decrease in fexofenadine blood exposure after treatment with SJW extract (Figure 4b), which is in good agreement with results from previous studies[6,7,36] and confirms the ability of the employed SJW extract to induce intestinal P-gp. The decrease in fexofenadine AUC observed in our study at end of treatment with SJW extract (−45%) was of similar magnitude as the decrease in fexofenadine AUC measured after treatment of healthy volunteers with rifampicin (600 mg/day) for 7 days (−48%).[20] Other than P-gp induction, we obtained evidence for induction of

17528062, 2024, 5, Downloaded from https://ascpt.onlinelibrary.wiley.com/doi/10.1111/cts.13804 by Bibliotheque de l'Universite de Geneve, Division de l'Information, Wiley Online Library on [26/06/2024]. See the Terms and Conditions (https://onlinelibrary.wiley.com/terms-and-conditions) on Wiley Online Library for rules of use; OA articles are governed by the applicable Creative Commons License

TABLE 1 Outcome parameters from kinetic modeling at baseline and after treatment with St. John's wort extract.

Brain region	Group	K_1 (mL/(cm^3 × min))	k_2 (1/min)	V_T (mL/cm^3)	V_b
Whole brain gray matter	Baseline	0.069 ± 0.009 (1–5)	0.039 ± 0.008 (2–11)	1.79 ± 0.23 (2–8)	0.029 ± 0.006 (2–13)
	St. John's wort	0.071 ± 0.012 (1–3)	0.040 ± 0.004 (2–6)	1.76 ± 0.27 (1–4)	0.031 ± 0.004 (2–6)
Cerebellum	Baseline	0.080 ± 0.012 (1–6)	0.048 ± 0.010 (2–12)	1.69 ± 0.24 (2–9)	0.037 ± 0.010 (2–17)
	St. John's wort	0.081 ± 0.015 (1–3)	0.049 ± 0.008 (2–6)	1.69 ± 0.28 (1–5)	0.037 ± 0.012 (2–5)
Middle frontal gyrus	Baseline	0.070 ± 0.010 (1–5)	0.038 ± 0.007 (2–10)	1.88 ± 0.21 (2–8)	0.022 ± 0.006 (3–28)
	St. John's wort	0.071 ± 0.011 (1–3)	0.039 ± 0.005 (2–6)	1.81 ± 0.27 (1–4)	0.022 ± 0.004 (2–9)
Basal ganglia	Baseline	0.071 ± 0.007 (1–4)	0.035 ± 0.007 (2–9)	2.10 ± 0.35 (1–6)	0.025 ± 0.006 (2–15)
	St. John's wort	0.073 ± 0.011 (1–3)	0.037 ± 0.004 (2–7)	2.00 ± 0.33 (1–5)	0.028 ± 0.009 (2–6)

Note: Values are reported as mean ± standard deviation. The values in parentheses represent the precision of the parameter estimates (expressed as range of standard error in percent). K_1 (mL/(cm^3 × min)), rate constant for radioactivity transfer from plasma into brain; k_2 (1/min), rate constant for radioactivity transfer from brain into plasma; V_T (mL/cm^3), total volume of distribution; V_b, fractional arterial blood volume in the brain.

CYP3A activity (measured as the 1-hydroxymidazolam/midazolam metabolic ratio) and CYP2C19 activity (measured as the 5-hydroxyomeprazole/omeprazole metabolic ratio) (Figure S1), which is also in good agreement with findings from previous studies.[37–39] In line with previous results,[37,39] treatment with SJW extract did not induce CYP2D6 activity (measured as the dextrorphan/dextromethorphan metabolic ratio), which was consistent with the lack of an effect on [^{11}C]metoclopramide metabolism.

For phenotyping, the cocktail was administered in the morning of each PET study day with a mean interval between cocktail administration and [^{11}C]metoclopramide injection of approximately 6 h. In vitro data suggest that midazolam[40] and omeprazole[41] may possess some P-gp inhibitory effect. However, the in vitro half-maximum inhibitory concentration (IC_{50}) values for P-gp inhibition (midazolam: >50 μmol/L, omeprazole: 17.7 μmol/L)[40,41] are far greater than the respective plasma concentrations measured in our study (midazolam: ~4 nmol/L, omeprazole: ~70 nmol/L), making P-gp inhibition at the BBB highly unlikely. Six subjects underwent [^{11}C]metoclopramide baseline PET scans for which the cocktail was not administered on the day of the PET scan but on another day after the PET scan. Figure S2 compares outcome parameters from kinetic modeling between baseline scans without and with cocktail administration, which revealed no significant differences and supports a lack of a P-gp-mediated interaction between the cocktail drugs and [^{11}C]metoclopramide at the BBB.

For the analysis of the brain distribution of [^{11}C]metoclopramide, we included WBGM, cerebellum, middle frontal gyrus, and basal ganglia as representative regions of interest. The latter were analyzed as dopamine D_2 receptor inhibition in the basal ganglia causes CNS-side effects of the antiemetic drug metoclopramide.[42] We used a 1T2K model to analyze the brain distribution of [^{11}C]metoclopramide.[17] We have shown in a previous study in healthy volunteers that V_T of [^{11}C]metoclopramide increased by 29% following P-gp inhibition with cyclosporin A.[17] This increase in V_T (= K_1/k_2) was due to both a decrease in k_2 and an increase in K_1, whereby the k_2 decrease was more pronounced than the K_1 increase. On the contrary, P-gp induction is expected to lead to an increase in k_2 and a decrease in V_T. While K_1 and probably also k_2 are perfusion-dependent,[43,44] V_T can be considered independent of cerebral blood flow (CBF). We performed no measurements of CBF in our study. There was a washout period of 46 ± 8 h between intake of the last SJW dose and administration of [^{11}C]metoclopramide, which makes an effect of SJW on CBF unlikely. None of the outcome parameters was significantly changed in any of the examined brain regions following treatment with SJW extract (Figure 3, Table 1).

A previous study used PET with racemic [^{11}C]verapamil to study the effect of oral treatment with rifampicin (600 mg/day) for 11–29 days on P-gp activity at the BBB of healthy volunteers.[43] Since rifampicin increased the CYP3A-mediated metabolism of [^{11}C]verapamil, only the first 5 min of the PET data following [^{11}C]verapamil injection were analyzed, during which the effect of rifampicin on [^{11}C]verapamil metabolism was minimal.[43] Similar to our results, the study found no changes in [^{11}C]verapamil brain distribution following treatment with rifampicin. However, data in a rat epilepsy model[45] and in human epilepsy patients[46] indicated that (*R*)-[^{11}C]verapamil lacks sensitivity to detect a seizure-induced P-gp upregulation in the brain, unless it is used under conditions of partial P-gp inhibition. It is therefore not entirely clear whether the failure to detect P-gp induction at the human BBB following treatment with rifampicin was due to a lack of sensitivity of [^{11}C]

17528062, 2024, 5, Downloaded from https://ascpt.onlinelibrary.wiley.com/doi/10.1111/cts.13804 by Bibliotheque de l'Universite de Geneve, Division de l'Information, Wiley Online Library on [26/06/2024]. See the Terms and Conditions (https://onlinelibrary.wiley.com/terms-and-conditions) on Wiley Online Library for rules of use; OA articles are governed by the applicable Creative Commons License

TABLE 2 Hyperforin plasma concentrations (ng/mL) in individual subjects at half time and at the end of treatment with St. John's wort extract and at the time of the second PET scan.

Subject	Duration of treatment with SJW (days)	Half	End	2nd PET scan[a]
01	13	24.1 (7)	–	24.3
02	15	104.8 (8)	117.8 (14)	30.4
03	13	112.8 (7)	180.1 (13)	21.2
04	19	65.2 (8)	179.3 (15)	22.1
05	17	34.7 (8)	181.9 (17)	14.6
06	15	79.8 (8)	321.4 (15)	37.8
07	13	91.2 (7)	243.0 (13)	12.3
08	14	286.6 (7)	361.6 (14)	26.0
09	16	91.4 (7)	111.4 (16)	16.6
10	12	80.5 (8)	94.8 (12)	23.6

Note: The value in parentheses represents the day after start of treatment with St. John's wort extract, when the blood sample was obtained.

[a]Second PET scan was performed 2 days after end of treatment with St. John's wort extract.

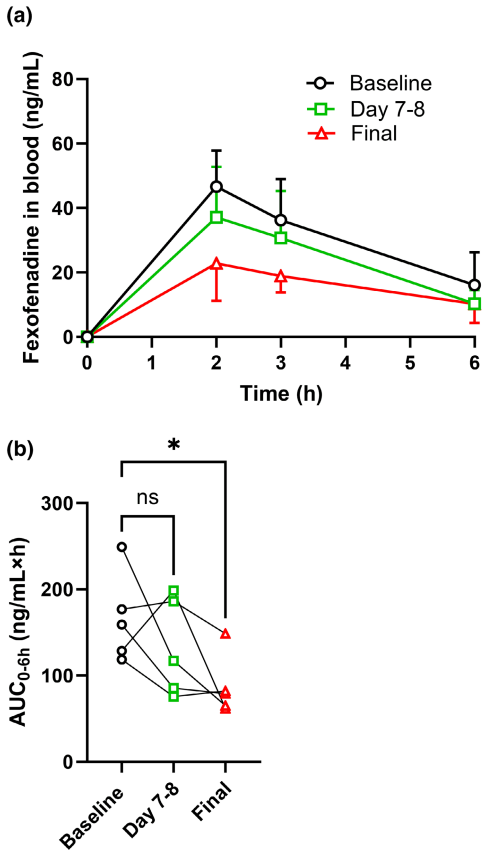

FIGURE 4 Concentration-time curves (mean ± SD, $n = 5$, a) and area under the curve values calculated from 0 to 6 h ($AUC_{0\text{-}6h}$, ng/mL × h, b) of the P-gp probe substrate fexofenadine in capillary dried blood spots after administration of the phenotyping cocktail at baseline (black circles), at day 7–8 (green squares) and after the end of treatment (red triangles) with St. John's wort extract. *$p \leq 0.05$; one-way ANOVA followed by a Dunnett's multiple comparison test against the baseline group.

verapamil or a lack of P-gp induction.[43] However, combined with our present results, it appears unlikely that a clinically relevant induction of P-gp activity can be achieved in vivo at the human BBB following treatment with the prototypical human PXR activators SJW or rifampicin. One possible explanation may be that the unbound hyperforin plasma concentrations were too low to activate PXR at the human BBB (see above). Another possible explanation may be that the abundance of PXR is considerably lower in human than in rodent brain capillary endothelial cells, so that P-gp activity cannot be induced at the human BBB.[43,47] However, this is not in line with another study, in which mRNA and protein expression of PXR was detected in an immortalized human cerebral microvessel endothelial cell line (hCMEC/D3) and in primary cultures of human brain-derived microvascular endothelial cells, and exposure to rifampicin was found to lead to a moderate increase in P-gp mRNA expression.[48] Another possible explanation may be related to poor BBB permeability of hyperforin resulting in insufficient intracellular hyperforin concentrations for PXR activation.[49] While rifampicin is a substrate of P-gp, which could limit its intracellular accumulation in brain capillary endothelial cells,[50] the P-gp substrate status of hyperforin is unknown. In contrast, hyperforin concentrations in the intestine and liver may have been much higher than in brain capillary endothelial cells resulting in effective peripheral P-gp and CYP enzyme induction.

P-gp has been implicated in the clearance of neurotoxic Aβ peptides from the brain and pharmacological induction of P-gp activity has been proposed as a therapeutic strategy to restore BBB functionality and enhance brain Aβ clearance in Alzheimer's disease patients.[11] Based on

17528062, 2024, 5, Downloaded from https://ascpt.onlinelibrary.wiley.com/doi/10.1111/cts.13804 by Bibliotheque de l'Universite de Geneve, Division de l'Information, Wiley Online Library on [26/06/2024]. See the Terms and Conditions (https://onlinelibrary.wiley.com/terms-and-conditions) on Wiley Online Library for rules of use; OA articles are governed by the applicable Creative Commons License

our current and previous data,[43] it appears unlikely that PXR activation at the human BBB can be therapeutically exploited to clear endogenous neurotoxic compounds, such as Aβ peptides, from the brain.

In conclusion, a combined approach involving PET imaging and cocktail phenotyping revealed that treatment with SJW extract with a high hyperforin content does not induce P-gp activity at the human BBB, despite effective induction of peripheral P-gp and CYPs. Simultaneous intake of SJW with CNS-targeted P-gp substrate drugs is not expected to lead to P-gp-mediated drug interactions at the BBB.

AUTHOR CONTRIBUTIONS

O.L. wrote the manuscript; M.W.-D., M.E.B., I.R., W.J., N.T., M.H., M.Z., M.B., and O.L designed the research; M.W.-D., M.J., M.E.B., S.M., M.W., K.B., S.P., N.S., L.N., and M.B. performed the research; M.E.B., S.M., S.P., I.R., I.H.L., and O.L. analyzed the data.

ACKNOWLEDGMENTS

The authors would like to thank Harald Ibeschitz and the other staff members of the PET center at the Division of Nuclear Medicine for their smooth cooperation in this study. Dr. Youssef Daali (Geneva University Hospitals, Geneva, Switzerland) is gratefully acknowledged for performing the dried blood spot analysis of the phenotyping cocktail drugs. Dr. Willmar Schwabe GmbH & Co. KG is acknowledged for providing the study medication.

FUNDING INFORMATION

This research was funded in part by the Austrian Science Fund (FWF) (grants KLI 694-B30 and I4470-B) and the Agence nationale de la recherche (ANR-19-CE17-0027). For open access purposes, the authors have applied a CC BY public copyright license to any author-accepted manuscript version arising from this submission.

CONFLICT OF INTEREST STATEMENT

The authors declared no competing interests for this work. This study was an investigator-initiated trial, for which Dr. Willmar Schwabe GmbH & Co. KG (Karlsruhe, Germany) provided the study medication (Neuroplant® tablets) free of charge. Dr. Willmar Schwabe GmbH & Co. KG had no influence on the design, conduct or the reporting of the study.

ORCID

Karsten Bamminger https://orcid.org/0000-0003-3811-7485
Ivo Rausch https://orcid.org/0000-0002-4007-1669
Oliver Langer https://orcid.org/0000-0002-4048-5781

REFERENCES

1. Linde K, Berner MM, Kriston L. St John's wort for major depression. *Cochrane Database Syst Rev*. 2008;2008:CD000448.
2. Nicolussi S, Drewe J, Butterweck V, Meyer Z, Schwabedissen HE. Clinical relevance of St. John's wort drug interactions revisited. *Br J Pharmacol*. 2020;177:1212-1226.
3. Moore LB, Goodwin B, Jones SA, et al. St. John's wort induces hepatic drug metabolism through activation of the pregnane X receptor. *Proc Natl Acad Sci USA*. 2000;97:7500-7502.
4. Mai I, Bauer S, Perloff ES, et al. Hyperforin content determines the magnitude of the St John's wort-cyclosporine drug interaction. *Clin Pharmacol Ther*. 2004;76:330-340.
5. Mueller SC, Uehleke B, Woehling H, et al. Effect of St John's wort dose and preparations on the pharmacokinetics of digoxin. *Clin Pharmacol Ther*. 2004;75:546-557.
6. Wang Z, Hamman MA, Huang SM, Lesko LJ, Hall SD. Effect of St John's wort on the pharmacokinetics of fexofenadine. *Clin Pharmacol Ther*. 2002;71:414-420.
7. Dresser GK, Schwarz UI, Wilkinson GR, Kim RB. Coordinate induction of both cytochrome P4503A and MDR1 by St John's wort in healthy subjects. *Clin Pharmacol Ther*. 2003;73:41-50.
8. Dürr D, Stieger B, Kullak-Ublick GA, et al. St John's wort induces intestinal P-glycoprotein/MDR1 and intestinal and hepatic CYP3A4. *Clin Pharmacol Ther*. 2000;68:598-604.
9. Doran A, Obach RS, Smith BJ, et al. The impact of P-glycoprotein on the disposition of drugs targeted for indications of the central nervous system: evaluation using the MDR1A/1B knockout mouse model. *Drug Metab Dispos*. 2005;33:165-174.
10. Bauer B, Hartz AM, Fricker G, Miller DS. Pregnane X receptor up-regulation of P-glycoprotein expression and transport function at the blood-brain barrier. *Mol Pharmacol*. 2004;66:413-419.
11. Hartz AM, Miller DS, Bauer B. Restoring blood-brain barrier P-glycoprotein reduces brain amyloid-beta in a mouse model of Alzheimer's disease. *Mol Pharmacol*. 2010;77:715-723.
12. Ott M, Fricker G, Bauer B. Pregnane X receptor (PXR) regulates P-glycoprotein at the blood-brain barrier: functional similarities between pig and human PXR. *J Pharmacol Exp Ther*. 2009;329:141-149.
13. Chan GN, Saldivia V, Yang Y, Pang H, de Lannoy I, Bendayan R. In vivo induction of P-glycoprotein expression at the mouse blood-brain barrier: an intracerebral microdialysis study. *J Neurochem*. 2013;127:342-352.
14. Jones SA, Moore LB, Shenk JL, et al. The pregnane X receptor: a promiscuous xenobiotic receptor that has diverged during evolution. *Mol Endocrinol*. 2000;14:27-39.
15. Zamek-Gliszczynski MJ, Patel M, Yang X, et al. Intestinal P-gp and putative hepatic OATP1B induction: international transporter consortium perspective on drug development implications. *Clin Pharmacol Ther*. 2021;109:55-64.
16. Bauer M, Tournier N, Langer O. Imaging P-glycoprotein function at the blood-brain barrier as a determinant of the variability in response to central nervous system drugs. *Clin Pharmacol Ther*. 2019;105:1061-1064.
17. Tournier N, Bauer M, Pichler V, et al. Impact of P-glycoprotein function on the brain kinetics of the weak substrate ^{11}C-metoclopramide assessed with PET imaging in humans. *J Nucl Med*. 2019;60:985-991.

17528062, 2024, 5, Downloaded from https://ascpt.onlinelibrary.wiley.com/doi/10.1111/cts.13804 by Bibliotheque de l'Universite de Geneve, Division de l'Information, Wiley Online Library on [26/06/2024]. See the Terms and Conditions (https://onlinelibrary.wiley.com/terms-and-conditions) on Wiley Online Library for rules of use; OA articles are governed by the applicable Creative Commons License

18. Pichler V, Ozenil M, Bamminger K, et al. Pitfalls and solutions of the fully-automated radiosynthesis of [^{11}C]metoclopramide. *EJNMMI Radiopharm Chem*. 2019;4:31.
19. Ott M, Huls M, Cornelius MG, Fricker GS. John's wort constituents modulate P-glycoprotein transport activity at the blood-brain barrier. *Pharm Res*. 2010;27:811-822.
20. Bosilkovska M, Samer CF, Déglon J, et al. Geneva cocktail for cytochrome p450 and P-glycoprotein activity assessment using dried blood spots. *Clin Pharmacol Ther*. 2014;96:349-359.
21. Sasongko L, Link JM, Muzi M, et al. Imaging P-glycoprotein transport activity at the human blood-brain barrier with positron emission tomography. *Clin Pharmacol Ther*. 2005;77:503-514.
22. Kreisl WC, Bhatia R, Morse CL, et al. Increased permeability-glycoprotein inhibition at the human blood-brain barrier can be safely achieved by performing PET during peak plasma concentrations of tariquidar. *J Nucl Med*. 2015;56:82-87.
23. Bauer M, Zeitlinger M, Karch R, et al. Pgp-mediated interaction between (*R*)-[^{11}C]verapamil and tariquidar at the human blood-brain barrier: a comparison with rat data. *Clin Pharmacol Ther*. 2012;91:227-233.
24. Mossel P, Garcia Varela L, Arif WM, et al. Evaluation of P-glycoprotein function at the blood-brain barrier using [^{18}F] MC225-PET. *Eur J Nucl Med Mol Imaging*. 2021;48:4105-4106.
25. Luurtsema G, Molthoff CF, Schuit RC, Windhorst AD, Lammertsma AA, Franssen EJ. Evaluation of (*R*)-[^{11}C]verapamil as PET tracer of P-glycoprotein function in the blood-brain barrier: kinetics and metabolism in the rat. *Nucl Med Biol*. 2005;32:87-93.
26. Desta Z, Wu GM, Morocho AM, Flockhart DA. The gastroprokinetic and antiemetic drug metoclopramide is a substrate and inhibitor of cytochrome P450 2D6. *Drug Metab Dispos*. 2002;30:336-343.
27. Glaeser H, Drescher S, Eichelbaum M, Fromm MF. Influence of rifampicin on the expression and function of human intestinal cytochrome P450 enzymes. *Br J Clin Pharmacol*. 2005;59:199-206.
28. Breuil L, Ziani N, Leterrier S, et al. Impact of cytochrome induction or inhibition on the plasma and brain kinetics of [^{11}C] metoclopramide, a PET probe for P-glycoprotein function at the blood-brain barrier. *Pharmaceutics*. 2022;14:2650.
29. Pottier G, Marie S, Goutal S, et al. Imaging the impact of the P-glycoprotein (ABCB1) function on the brain kinetics of metoclopramide. *J Nucl Med*. 2016;57:309-314.
30. Feng B, Mills JB, Davidson RE, et al. In vitro P-glycoprotein assays to predict the in vivo interactions of P-glycoprotein with drugs in the central nervous system. *Drug Metab Dispos*. 2008;36:268-275.
31. Zoufal V, Mairinger S, Brackhan M, et al. Imaging P-glycoprotein induction at the blood-brain barrier of a beta-amyloidosis mouse model with ^{11}C-metoclopramide PET. *J Nucl Med*. 2020;61:1050-1057.
32. Anghelescu IG, Kohnen R, Szegedi A, Klement S, Kieser M. Comparison of hypericum extract WS 5570 and paroxetine in ongoing treatment after recovery from an episode of moderate to severe depression: results from a randomized multicenter study. *Pharmacopsychiatry*. 2006;39:213-219.
33. Biber A, Fischer H, Römer A, Chatterjee SS. Oral bioavailability of hyperforin from hypericum extracts in rats and human volunteers. *Pharmacopsychiatry*. 1998;31(Suppl 1):36-43.
34. Adiwidjaja J, Boddy AV, McLachlan AJ. Physiologically based pharmacokinetic modelling of hyperforin to predict drug interactions with St John's wort. *Clin Pharmacokinet*. 2019;58:911-926.
35. Kalvass JC, Polli JW, Bourdet DL, et al. Why clinical modulation of efflux transport at the human blood-brain barrier is unlikely: the ITC evidence-based position. *Clin Pharmacol Ther*. 2013;94:80-94.
36. Xie R, Tan LH, Polasek EC, et al. CYP3A and P-glycoprotein activity induction with St. John's wort in healthy volunteers from 6 ethnic populations. *J Clin Pharmacol*. 2005;45:352-356.
37. Wang Z, Gorski JC, Hamman MA, Huang SM, Lesko LJ, Hall SD. The effects of St John's wort (*Hypericum perforatum*) on human cytochrome P450 activity. *Clin Pharmacol Ther*. 2001;70:317-326.
38. Wang LS, Zhou G, Zhu B, et al. St John's wort induces both cytochrome P450 3A4-catalyzed sulfoxidation and 2C19-dependent hydroxylation of omeprazole. *Clin Pharmacol Ther*. 2004;75:191-197.
39. Gurley BJ, Gardner SF, Hubbard MA, et al. Cytochrome P450 phenotypic ratios for predicting herb-drug interactions in humans. *Clin Pharmacol Ther*. 2002;72:276-287.
40. Schwab D, Fischer H, Tabatabaei A, Poli S, Huwyler J. Comparison of in vitro P-glycoprotein screening assays: recommendations for their use in drug discovery. *J Med Chem*. 2003;46:1716-1725.
41. Pauli-Magnus C, Rekersbrink S, Klotz U, Fromm MF. Interaction of omeprazole, lansoprazole and pantoprazole with P-glycoprotein. *Naunyn Schmiedeberg's Arch Pharmacol*. 2001;364:551-557.
42. Bauer M, Bamminger K, Pichler V, et al. Impaired clearance from the brain increases the brain exposure to metoclopramide in elderly subjects. *Clin Pharmacol Ther*. 2021;109:754-761.
43. Liu L, Collier AC, Link JM, et al. Modulation of P-glycoprotein at the human blood-brain barrier by quinidine or rifampin treatment: a PET imaging study. *Drug Metab Dispos*. 2015;43:1795-1804.
44. Kreisl WC, Liow JS, Kimura N, et al. P-glycoprotein function at the blood-brain barrier in humans can be quantified with the substrate radiotracer ^{11}C-N-desmethyl-loperamide. *J Nucl Med*. 2010;51:559-566.
45. Bankstahl JP, Bankstahl M, Kuntner C, et al. A novel PET imaging protocol identifies seizure-induced regional overactivity of P-glycoprotein at the blood-brain barrier. *J Neurosci*. 2011;31:8803-8811.
46. Feldmann M, Asselin MC, Liu J, et al. P-glycoprotein expression and function in patients with temporal lobe epilepsy: a case-control study. *Lancet Neurol*. 2013;12:777-785.
47. Dauchy S, Dutheil F, Weaver RJ, et al. ABC transporters, cytochromes P450 and their main transcription factors: expression at the human blood-brain barrier. *J Neurochem*. 2008;107:1518-1528.
48. Chan GN, Hoque MT, Cummins CL, Bendayan R. Regulation of P-glycoprotein by orphan nuclear receptors in human brain microvessel endothelial cells. *J Neurochem*. 2011;118:163-175.

17520062, 2024, 5, Downloaded from https://ascpt.onlinelibrary.wiley.com/doi/10.1111/cts.13804 by Bibliotheque de l'Universite de Geneve, Division de l'Information, Wiley Online Library on [26/06/2024]. See the Terms and Conditions (https://onlinelibrary.wiley.com/terms-and-conditions) on Wiley Online Library for rules of use; OA articles are governed by the applicable Creative Commons License

49. Caccia S, Gobbi MS. John's wort components and the brain: uptake, concentrations reached and the mechanisms underlying pharmacological effects. *Curr Drug Metab*. 2009;10:1055-1065.
50. Spudich A, Kilic E, Xing H, et al. Inhibition of multidrug resistance transporter-1 facilitates neuroprotective therapies after focal cerebral ischemia. *Nat Neurosci*. 2006;9:487-488.

SUPPORTING INFORMATION

Additional supporting information can be found online in the Supporting Information section at the end of this article.

How to cite this article: El Biali M, Wölfl-Duchek M, Jackwerth M, et al. St. John's wort extract with a high hyperforin content does not induce P-glycoprotein activity at the human blood–brain barrier. *Clin Transl Sci*. 2024;17:e13804. doi:10.1111/cts.13804

17528062, 2024, 5, Downloaded from https://ascpt.onlinelibrary.wiley.com/doi/10.1111/cts.13804 by Bibliotheque de l'Universite de Geneve, Division de l'Information, Wiley Online Library on [26/06/2024]. See the Terms and Conditions (https://onlinelibrary.wiley.com/terms-and-conditions) on Wiley Online Library for rules of use; OA articles are governed by the applicable Creative Commons License